EUROPEAN MECHANICAL SCIENCE
e-ISSN: 2587-1110

RESEARCH ARTICLE

Finite element analysis of the seepage problem in the dam body and foundation based on the Galerkin's approach

Timuçin Alp Aslan[1*], Beytullah Temel[1]

[1]Cukurova University, Department of Civil Engineering, Adana, Turkey

Orcid: T.A.Aslan (0000-0002-7558-3568), B. Temel (0000-0002-1673-280X)

Abstract: In this study, the 2D steady-state seepage analysis of the dam body and its base is investigated using the finite element method (FEM) based on Galerkin's approach. The body and foundation soil is considered as homogeneous isotropic and anisotropic materials and the effects of horizontal drainage length and the cutoff wall on seepage are investigated. The differential equation governing the response of water in the soil is obtained with the help of Darcy's law and continuity equations. A program has been prepared in Fortran programming language to find the hydraulic load, pressure values and phreatic line pressure values at the points inside the dam body and the quantity of seepage on the bottom of dam. It has been shown that the obtained values are in good agreement by comparing them with the results of existing studies in the literature.

Keywords: Dam; Seepage analysis; Finite element methods, Phreatic line, Hydraulic head

1. Introduction

As with many engineering problems, the state and movement of water in the body and foundation ground of impounding dams need to be analyzed. Seepage; It is the uncontrolled, unmeasurable continuous movement of water accumulated in the upstream part of the dam towards the downstream part. Seepage in the bodies of the dams causes water loss from the reservoir, as well as erosion in the fill, causing piping to occur. This situation causes damage to the dam's body and may even cause the dam to collapse. For these reasons, seepage problems in the dam body and its foundation continue to be a current issue and are being investigated by many researchers. Ardıçlıoğlu [1] used the FEM for the analysis of the 2D steady-state seepage analysis of the embankment dam body and calculated the pore water pressures of the element nodes in the flow regions and the seepage rate through the unit width of the embankment. Keskin [2] studied the potential and velocity distributions of various sheet piles, spillways, and earth-fill dams in the body and bottom of the seepage in two dimensions using the FEM. Çilingir [3] investigated the seepage in the body of Büyükçekmece dam, which was chosen as a mathematical model, by using the FEM and the Geo-Studio computer program. Fakhari and Ghanbari [4] developed a new formula to find the total amount of seepage through a clay core dam body and compared it with all other flow calculation methods. Çelik [5] performed a two-dimensional seepage analysis on the Ikizdere Dam body cross-sections with the Seep/W program. In the selection of the material parameters of the model entered into the program, the laboratory test results presented in the project sheets and the literature were used. Sağlıca [6] wrote a program that performs seepage analysis with the finite difference method (FDM) and compared the values found as a result of the analysis with the results obtained by other methods. Darbandi et al. [7] developed A Moving-Mesh finite volume method (FVM) that can solve the seepage problem in arbitrary geometries. Rafiezadeh and Ataie-Ashtiani [8] improved the three-dimensional boundary element solution based on the transformation approach for the analysis of seepage in a multi-domain general anisotropic media. Ouria and Toufigh [9] used the FEM based on Nelder-Mead simple optimization and the changing mesh technique to solve the unconfined seepage problems. El-Jumaily and Al-Bakry [10] examined the seepage analysis through and underneath the hydraulic structures together without dividing the structure into parts, and then analyzed it with the FVM using rectangular elements separately for each of the parts. Mesci [11] investigated the methods used to determine the seepage occurring in the dam bodies and calculated the total seepage amounts by determining the flow of water in the dam body with these meth-

*Corresponding author.
Email: taslan@cu.edu.tr

European Mechanical Science (2022), 6(2): 143-151
https://doi.org/10.26701/ems.1024266
Received: November 16, 2021 — Accepted: March 16, 2022

ods. Çakır [12] sophisticated a numerical model for the two-dimensional groundwater flow using the collocation method. For the purpose of comparison, they prepared a MATLAB program with the FDM. Quanshu and Jianjun [13] adopted a numerical simulation method for leakage analysis and investigated the influence of core and other factors by comparing the leakage area under different conditions. Mansuri and Salmasi [14] focused on the effectiveness of using horizontal drainage and cutoff wall in reducing seepage flow from a heterogeneous earth dam. For this purpose, they investigated the effect of various horizontal drainage lengths and shear wall depths on seepage under the earth dam at different locations of the foundation. Sakhmarsi et al. [15] investigated the influence of cutoff wall depth, position, and permeability properties on seepage in the homogeneous earth-fill dams using SEEP/W computer software. Yuan and Zhong[16] used the weak-form quadrature element method for the analysis of three-dimensional unconstrained seepage problems. Zhang et al. [17] proposed a moving kriging mesh-free method with Monte Carlo integration to determine the phreatic surface while investigating the seepage analysis. Khassaf and Madhloom [18] found the quantity of seepage that occurs in soil dams with the effect of changing the core permeability and the core thickness of a core region by using the FEM SLIDE V.5.0 software. Zewdu[19], calculated the amount of the seepage occurring in the Koga earth-fill dam body and foundation using the finite element-based PLAXIS 2D software. Taghvaei et al. [20] prepared numerical modeling of earth dam in different clay-sand compositions using SEEP/W software and validated it with experimental results. In their paper, Doaa and Molla [21] aimed to determine the effect of the existence of the sheet pile as well as its height and location on the total seepage discharge and velocities through the dam's cross-section. Sanayei and Javdanian [22] developed a new analytical solution for steady seepage from dams with nonsymmetric boundary conditions. Non-symmetrical boundary conditions for two-dimensional cases were created in dams with different unit step functions in the downstream part of the dam plane. Salmasi et al. [23] used the FEM to investigate the effect of the cutoff wall and downstream filters on seepage events occurring at the dam foundation and verified the experimental data with numerical modeling. Kheiri et al. [24] calculated the seepage under clay core embankment dams using the finite element based SEEP/W program and demonstrated the accuracy of their results by comparing them with the physical modeling results.

Preventing seepage in dam bodies is very difficult and requires great economic costs. For these reasons, it is important to calculate the amount of seepage that will occur by carrying out detailed research and studies during the design phase before the dam construction starts. In this study, the 2D steady-state seepage analysis of the embankment dam body and its base will be examined by the FEM. As it is known, the FEM is a numerical method used in the solution of engineering problems, especially in recent years, due to its many advantages [25-29]. The main purpose of this paper is to demonstrate the effective and easy usability of the FEM based on Galerkin's element approach in seepage problems in isotropic and anisotropic soil mediums. For the suggested models, a computer program is coded in Fortran for the steady-state seepage analysis. With the aid of the written program, different types of seepage problems can be solved efficiently and accurately.

2. MATHEMATICAL FORMULATIONS

2D steady-state seepage in a permeable, anisotropic soil (Figure 1) is expressed by the following partial differential equation with the help of Darcy's law and continuity equations [30].

$$K_x \frac{\partial^2 h}{\partial x^2} + K_y \frac{\partial^2 h}{\partial y^2} = 0 \quad (1)$$

where, K_x and K_y are the coefficients of hydraulic conductivity in the x and y direction, h is the total hydraulic head.

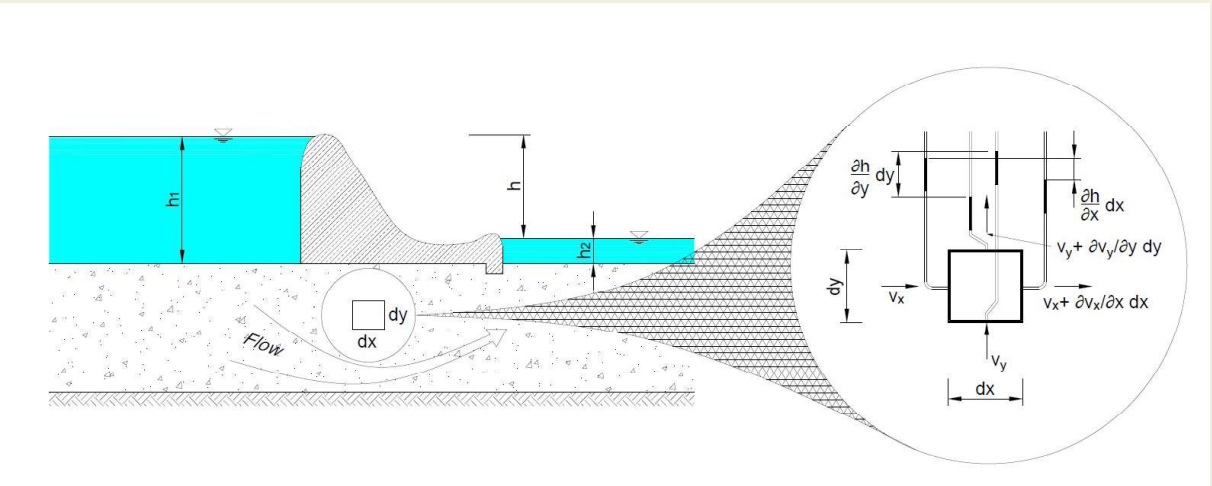

Figure 1. Flow of water through saturated pervious soil beneath a hydraulic structure

It is the sum of the elevation head and the pressure head as stated in the eq. (1). The velocity head is ignored due to the very slow movement of the water in the ground.

$$h = z + \frac{p}{\gamma_w} \tag{2}$$

The partial differential form of eq. (1) is written in integral form by applying the weighted residuals method as follows:

$$\int\int_{Ae} \psi \left(K_x \frac{\partial^2 h}{\partial x^2} + K_y \frac{\partial^2 h}{\partial y^2} \right) dA = 0 \tag{3}$$

Eq. (4) is obtained by the application of the partial integration to eq. (3).

$$\int\int_{Ae} \left(K_x \frac{\partial \psi}{\partial x}\left(\frac{\partial h}{\partial x}\right) + K_y \frac{\partial \psi}{\partial y}\left(\frac{\partial h}{\partial y}\right) \right) dxdy$$
$$- \int_{\Gamma} \psi \left(\frac{\partial h}{\partial x} n_x + \frac{\partial h}{\partial y} n_y \right) d\sigma = 0 \tag{4}$$

In these expressions, the second part represents the boundary conditions, Γ represents the boundary of the element, n_x and n_y are components of the unit vector, q is the inflow or the outflow of the unit boundary surface and σ is the integration variable along the boundary in the counterclockwise direction.

In the Galerkin method, the variation of the hydraulic load is taken into account as weight functions.

$$\psi = \delta h \tag{5}$$

Equation (6) is obtained by substituting the weight functions in eq. (4).

$$\int\int_{Ae} \left(K_x \frac{\partial(\delta h)}{\partial x}\left(\frac{\partial h}{\partial x}\right) + K_y \frac{\partial(\delta h)}{\partial y}\left(\frac{\partial h}{\partial y}\right) \right) dxdy - \int_{\Gamma} (\delta h) q d\sigma = 0 \tag{6}$$

FEM is one of the effective numerical methods. This approach divides the problem domain into several elements with limited sizes and gives approximate solutions for the nodes of the system. In this study, an isoparametric 8-noded serendipity element is used in the formulation. The hydraulic heads at any point of the element are given in eq. (7).

$$\{h\} = [N_1\ N_2\ N_3\ N_4\ N_5\ N_6\ N_7\ N_8] \begin{Bmatrix} h_1 \\ h_2 \\ h_3 \\ h_4 \\ h_5 \\ h_6 \\ h_7 \\ h_8 \end{Bmatrix} = [N]\{\Delta\} \tag{7}$$

where is $[N]$ the matrix of shape functions and $\{\Delta\}$ is the element hydraulic heads. The coordinates of any point in the quadratic element are given below depending on the shape functions.

$$x = \sum_{i=1}^{8} N_i x_i \qquad y = \sum_{i=1}^{8} N_i y_i \tag{8}$$

where x_i and y_i are the coordinates of a node. For isoparametric elements, the geometric shape functions and interpolation shape functions are the same. The hydraulic head at any point of the element can be calculated with the help of element node loads depending on the shape functions.

$$h(\xi,\eta) = \sum_{i=1}^{8} N_i(\xi,\eta)\ h_i \tag{9}$$

Substituting Eq. (7) into Eq. (6) gives the following equation

$$\int\int_{Ae} \left(\frac{\partial(\delta h)}{\partial x} K_x \left(\frac{\partial [N]\{\Delta\}}{\partial x} \right) + \frac{\partial(\delta h)}{\partial y} K_y \left(\frac{\partial [N]\{\Delta\}}{\partial y} \right) \right) dxdy - \int_{\Gamma} (\delta h)\ q\ d\sigma = 0 \tag{10}$$

Eq. (10) is based on the hydraulic head gradient vector and can be given as follows:

$$\{gv\} = \begin{Bmatrix} \frac{\partial h}{\partial x} \\ \frac{\partial h}{\partial y} \end{Bmatrix} = \begin{bmatrix} \frac{\partial [N]}{\partial x} \\ \frac{\partial [N]}{\partial y} \end{bmatrix} \{\Delta\} = [B]\{\Delta\} \tag{11}$$

Accordingly, the hydraulic head variations are expressed as follows.

$$\delta h = [N]\{\delta\Delta\}$$
$$\delta h^T = \{\delta\Delta\}^T [N]^T \tag{12}$$

Substituting of eqs. (11-12) into eq. (10) leads to,

$$\int\int_{Ae} \left(\frac{\partial [N]\{\delta\Delta\}}{\partial x} K_x \left(\frac{\partial [N]\{\Delta\}}{\partial x} \right) + \frac{\partial [N]\{\delta\Delta\}}{\partial y} K_y \left(\frac{\partial [N]\{\Delta\}}{\partial y} \right) \right) dxdy - \int_{\Gamma} [N]\{\delta\Delta\}\ q\ d\sigma = 0 \tag{13}$$

The simplified form of eq. (13) is given as:

$$\{\delta\Delta\}^T \left(\int\int_{Ae} \left([B]^T [K][B] \right) dA\{\Delta\} \right) - \int_{\Gamma} [N]^T q\ d\sigma = 0 \tag{14}$$

where $[K]$ is the conductivity matrix.

$$[K] = \begin{bmatrix} K_x & 0 \\ 0 & K_y \end{bmatrix} \tag{15}$$

The element stiffness matrix, $[s_e]$, and the element applied flux vector , $\{f_s\}$, are:

$$[s_e]_{(8*8)} = \int_{Ae}\int \left([B]^T [K][B]\right) dA$$

$$, \quad \{f_s\}_{(8*1)} = \int_{\Gamma}\left([N]^T q\right) d\sigma \tag{16}$$

The general form of finite element equation for steady state seepage analysis is:

$$[s_e]\{\Delta\} = \{f_s\} \tag{17}$$

where $\{\Delta\}$ is element hydraulic head vector. The value of $\{f_s\}$ is 0 (zero) at the nodes that are not on the boundary. In any flow region, the global conductance matrix and system hydraulic head vector are formed by taking the contribution of the elements.

$$[S]\{\Delta\} = \{F\} \tag{18}$$

where, $[S]$ is the global conductance matrix, $\{\Delta\}$ is the system hydraulic head vector and $\{F\}$ is the system load vector for all nodes. Under the specified boundary conditions, the total hydraulic head at the nodes is found by the numerical solution. Then, hydraulic gradients, flow velocities, the quantity of seepage and pressure values can be easily calculated.

In seepage problems, boundary conditions are used to solve the main differential equation of seepage. Boundary conditions are related to initial conditions and different flow patterns of the system. The boundary conditions do not depend on time under steady-state flow conditions. In this study, upstream and downstream levels are defined as constant head boundary conditions in order to model the seepage through the considered dams. A seepage line may be formed at the downstream region of the dam. Boundary conditions for seepage problems of the embankment dam with tailwater in the downstream region are given in Figure 2.

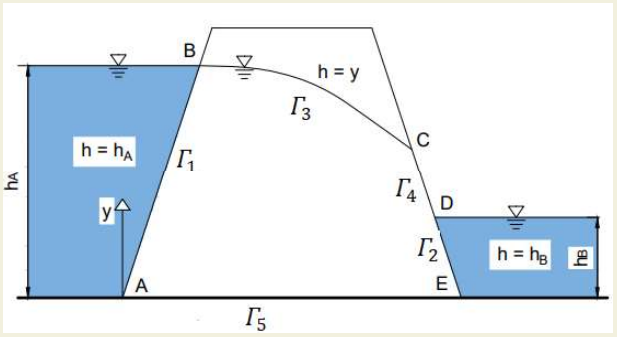

Figure 2. Seepage and boundary conditions in an embankment dam

Since the position of the phreatic surface BC in Figure 1 is not clear, it requires an iterative solution of the finite element analysis. First of all, the free surface estimated seepage line is determined, and a solution is made. After each iterative process, the free surface is updated by substituting the newly computed hydraulics heads to the old coordinates of the free surface. These processes are repeated until the error is the convergence criterion [31].

$h = h_A$ AB-Γ_1 (Upstream surface)

$h = h_B$ ED-Γ_2 (Downstream surface)

$\left\{\begin{matrix} h = y \\ \frac{\partial h}{\partial n} = 0 \end{matrix}\right\}$ BC-Γ_3 (Phreatic surface)

$h = y$ CD-Γ_4 (Seepage surface)

$\frac{\partial h}{\partial n} = 0$ AE-Γ_5 (Impervious surface)

2. Numerical Examples and Discussion

In this section, seepage analysis of dam bodies and foundations with different geometries and material properties has been studied. Element stiffness matrix and hydraulic head vector are calculated by the Gauss-Legendre numerical integral method. Several types of seepage problems are investigated with the programs written in Fortran using the FEM [32].

Example 1

Firstly, time indepented seepage phenomenon has been investigated in the homogeneous isotropic fill dam body. The material and geometrical properties are given in Figure 3.

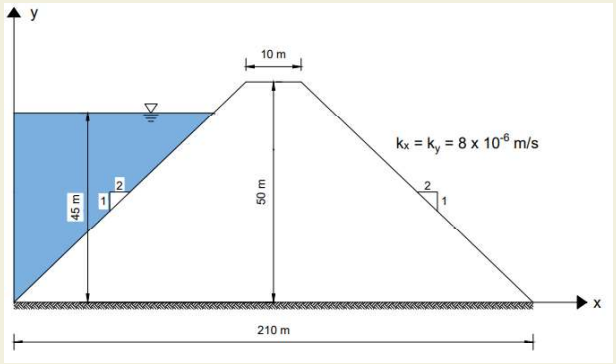

Figure 3. Geometry and material properties of the dam

The seepage value passing through the fill dam body, calculated by the FEM based on Galerkin's approach, is being compared with the results present in the literature in Table 1. It can be seen that the results are in a good agreement.

Table 1. Seepage rate per unit width of the dam ($m^3/s/m$)

Ardıçlıoğlu [1]	Flow Net Method [1]	Present Study
6.9803×10^{-5}	6.8572×10^{-5}	6.8478×10^{-5}

To perform the calculations, the seepage region is divided into 40 finite elements (149 nodes). The hydraulic head and pressure values of the embankment dam at the nodes indicated on Figure 4 are calculated and presented in Table 2.

Table 2. Hydraulic head and pressure load values of the dam

NODE	X (m)	Y (m)	HYDRAULIC HEAD (m)	PRESSURE HEAD (m)	NODE	X (m)	Y (m)	HYDRAULIC HEAD (m)	PRESSURE HEAD (m)
1	0.000	0.000	45.000	45.000	91	128.750	15.938	32.685	16.747
2	10.500	0.000	44.998	44.998	97	67.500	33.750	45.000	11.250
3	21.000	0.000	44.966	44.966	98	74.100	32.287	44.412	12.125
19	189.000	0.000	10.084	10.084	99	80.700	30.825	43.502	12.677
20	199.500	0.000	4.712	4.712	105	120.300	22.050	35.033	12.983
21	210.000	0.000	0.000	0.000	106	126.900	20.588	33.348	12.760
22	11.250	5.625	45.000	39.375	107	133.500	19.125	31.582	12.457
23	30.950	5.137	44.889	39.751	115	186.300	7.425	11.741	4.316
31	188.550	1.237	10.332	9.095	116	192.900	5.963	8.038	2.075
32	208.250	0.750	0.750	0.000	117	199.500	4.500	4.500	0.000
33	22.500	11.250	45.000	33.750	118	78.750	39.375	45.000	5.625
34	31.700	10.762	44.928	34.165	119	90.650	35.963	42.789	6.826
35	40.900	10.275	44.759	34.484	127	185.850	8.663	12.003	3.340
51	188.100	2.475	10.589	8.114	128	197.750	5.250	5.250	0.000
52	197.300	1.987	5.764	3.776	129	90.000	45.000	45.000	0.000
53	206.500	1.500	1.500	0.000	130	95.300	43.003	43.004	0.000
73	108.200	14.700	37.478	22.778	131	100.600	41.001	41.001	0.000
74	116.100	13.725	35.690	21.965	147	185.400	12.300	12.300	0.000
75	124.000	12.750	33.775	21.025	148	190.700	9.650	9.650	0.000
90	114.250	18.375	36.283	17.908	149	196.000	6.000	6.299	0.000

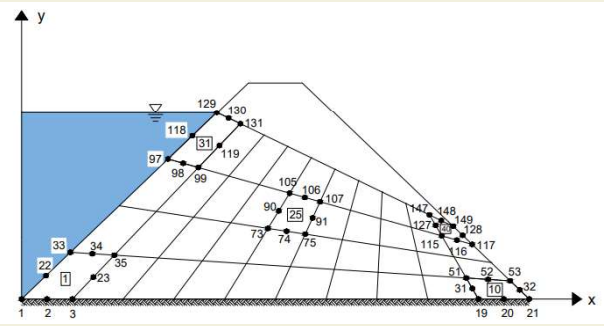

Figure 4. Finite element model of the dam

From Table 2, it can be clearly seen that the highest hydraulic head and pressure load values are in the region of the upstream part close to the foundation.

Example 2

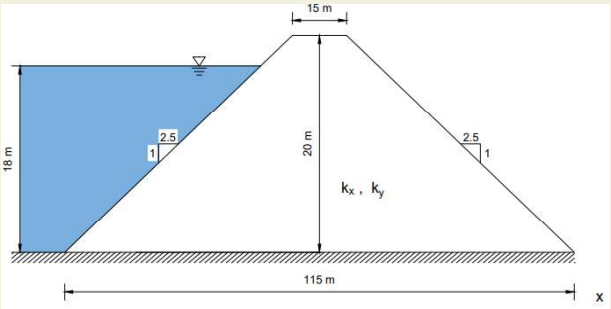

Figure 5. Geometry and material properties of the dam

The seepage quantity of dams in different situations with isotropic and anisotropic filling material properties are calculated and given in Table 3. The geometric properties of the dam are given in Figure 5.

Table 3. Seepage rate per unit width of dams with different soil properties ($m^3/s/m$)

	Permeability Coefficient (m/s)	Present Study
Case 1	$K_x = 4.5\ x\ 10^{-8}$ $K_y = 4.5\ x\ 10^{-8}$	$1.060903x\ 10^{-7}$
Case2	$K_x = 1.6\ x\ 10^{-8}$ $K_y = 4.5\ x\ 10^{-8}$	$0.3974995x\ 10^{-7}$
Case 3	$K_x = 4.5\ x\ 10^{-8}$ $K_y = 1.6\ x\ 10^{-8}$	$1.001256x\ 10^{-7}$

In Table 3, where different soil conditions are compared, it can be seen that the permeability coefficient in the x direction is more effective on seepage.

Example 3

For the embankment dam with anisotropic material (Figure 6), with horizontal drainage at the downstream part of the body, the unit width seepage rate has been calculated. The effect of the drainage length on the seepage has been investigated. The results are presented in Table 4.

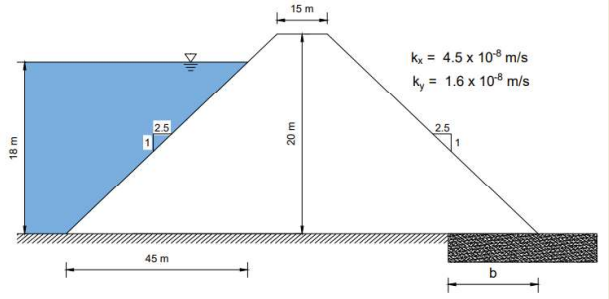

Figure 6. Geometry and material properties of the dam with horizontal drainage

Table 4. Seepage rate per unit width of dams with horizontal drainage of different lengths ($m^3/s/m$)

Horizontal Drain Length, b (m)	Sağlıca [6]	Present Study
15.5	$1.000x\ 10^{-7}$	$1.023x\ 10^{-7}$
18.0	-	$1.041x\ 10^{-7}$
21.0	-	$1.058x\ 10^{-7}$
25.0	-	$1.106x\ 10^{-7}$

Table 4 presents that the amount of seepage per unit width increases as the horizontal drainage length increases.

So that the rate of seepage increase for the length of the horizontal drains with 15.5, 18.0, 21.0 and 25.0 meters are 2.17%, 3.97%, 5.67% and 10%, respectively.

Also, for the horizontal undrained (Case 3) and horizontally drained embankment dams with anisotropic material, the location of the phreatic line is determined and shown in Figure 6.

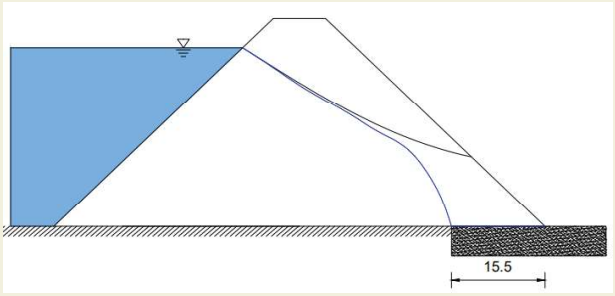

Figure 7. Phreatic line of the dam

It can be seen in Figure 7, that the seepage line in dams with horizontal drainage is inside the dam body and it cannot cause any possible damage to the downstream region due to piping. This result demonstrates the importance of using the horizontal drains to control the position of the phreatic line for the stability of earthen dams.

Example 4

In this example, the seepage amount has been calculated for the rectangular dam body with water in the downstream region. The geometric and material properties are given in Figure 8. The results obtained in this section are given in Table 5 and compared with those of Parsi and Daneshm [33] and Parsi [34]. They [33, 34] examine the position of the phreatic surface, which is unknown at the beginning of the solution and must be determined in an iterative process, with different theories.

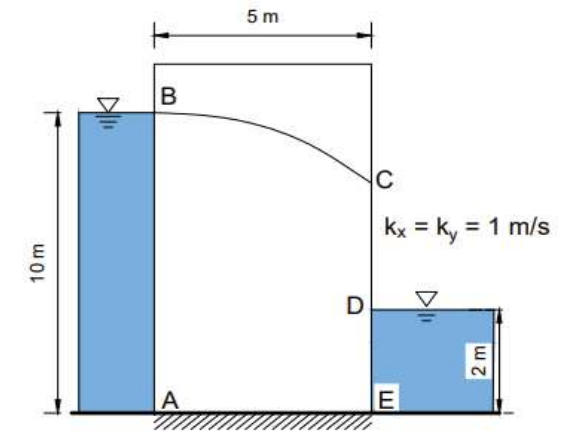

Figure 8. Geometry and material properties of the dam

In comparison with the current literature, it is seen that the seepage results given in Table 5 are in excellent agreement.

Table 5. Seepage rate per unit width of the dam ($m^3/s/m$)

Parsi and Daneshm [33]	Parsi [34]	Present Study
9.60	9.64	9.61

Example 5

The value of the seepage discharge through the foundation of the dam is calculated and given in Table 6. The geometric properties of the dam are illustrated in Figure 9. It has been seen that the results of the suggested approach are quite close to the result found in the literature.

Table 6. Seepage rate per unit width of the dam foundation ($m^3/s/m$)

Mansuri [35]	Present Study
$7.7015x\ 10^{-5}$	$7.6502x\ 10^{-5}$

While performing the calculations, the seepage region has been divided into 1250 finite element elements (3901 nodes). The hydraulic head and pressure values of the dam are calculated and shown in Table 7 at the points of the foundation ends and the middle (1,50,1200,1250) and the two elements (1221,1231) located under the body downstream and upstream region.

Several studies are carried out to reduce high uplift forces which is a result of water seeping when the foundation

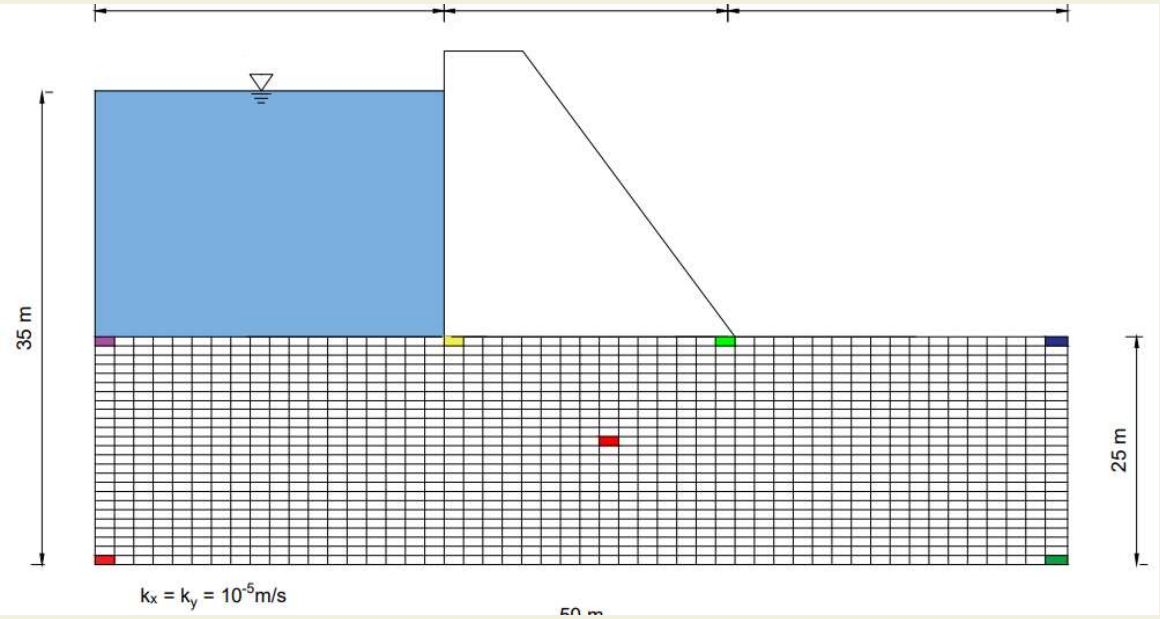

Figure 9. Geometry and material properties of the dam

Table 7. Hydraulic head and pressure load values of the dam

NODE	X (m)	Y (m)	HYDRAULIC HEAD (m)	PRESSURE HEAD (m)	NODE	X (m)	Y (m)	HYDRAULIC HEAD (m)	PRESSURE HEAD (m)
1	0.0	0.0	32.412	32.412	3690	20.5	24	33.279	9.279
2	0.5	0.0	32.410	32.410	3691	21.0	24	32.793	8.793
3	1.0	0.0	32.407	32.407	3709	30.0	24	26.359	2.359
99	49.0	0.0	27.520	27.520	3710	30.5	24	26.026	2.026
100	49.5	0.0	27.517	27.517	3711	31.0	24	25.847	1.847
101	50.0	0.0	27.516	27.516	3747	49.0	24	25.169	1.169
102	0.0	0.5	32.413	31.913	3748	49.5	24	25.169	1.169
103	1.0	0.5	32.408	31.908	3749	50.0	24	25.169	1.169
151	49	0.5	27.519	27.019	3750	0.0	24.5	34.912	10.412
152	50	0.5	27.515	27.015	3751	1.0	24.5	34.912	10.412
153	0.0	1.0	32.416	31.416	3770	20.0	24.5	34.137	9.637
154	0.5	1.0	32.415	31.415	3771	21.0	24.5	32.987	8.487
155	1.0	1.0	32.412	31.412	3780	30.0	24.5	25.853	1.353
251	49.0	1.0	27.516	26.516	3781	31.0	24.5	25.430	0.930
252	49.5	1.0	27.513	26.513	3799	49.0	24.5	25.085	0.585
253	50.0	1.0	27.512	26.512	3800	50.0	24.5	25.084	0.584
1873	24.0	12.0	30.198	18.198	3801	0.0.	25	35.000	10.000
1874	24.5	12.0	30.082	18.082	3802	0.5	25	35.000	10.000
1875	25.0	12.0	29.965	17.965	3803	1.0	25	35.000	10.000
1950	24.0	12.5	30.206	17.706	3841	20.0	25	35.000	10.000
1951	25.0	12.5	29.966	17.466	3842	20.5	25	33.756	8.756
2025	24.0	13.0	30.215	17.215	3843	21.0	25	32.986	7.986
2026	24.5	13.0	30.091	17.091	3861	30.0	25	25.000	0.000
2027	25.0	13.0	29.966	16.966	3862	30.5	25	25.000	0.000
3649	0.0	24.0	34.824	10.824	3863	31.0	25	25.000	0.000
3650	0.5	24.0	34.824	10.824	3899	49.0	25	25.000	0.000
3651	1.0	24.0	34.823	10.823	3900	49.5	25	25.000	0.000
3689	20	24.0	33.625	9.625	3901	50.0	25	25.000	0.000

with high permeability is used. This can pose a danger in hydraulic structures. So, the researchers and engineers try to reduce this undesired situation as much as possible. Thus, the stability of the dam can be ensured.

Example 6

In the last example, the effect of the cutoff wall shown in Figure 10 on the quantity of seepage from the dam foundation has been investigated. An impermeable cutoff wall with depths of 7, 8, 9, 10, 11, and 12 m has been installed at the upstream ends of the dam model. For a cutoff position at the upstream end of the dam, the rate of the seepage discharge from the foundation in the depth of 7- 12 m, the rate of seepage discharge reduction to the base model are 28.97%, 32.43%, 35.72%, 38.85%, 41.84%, and 44.69 % respectively. From Table 8 it can be understood that the cutoff wall has a significant effect on the seepage and the seepage decreases as its length increases.

Table 8. Seepage rate per unit width of dams with cuttoff wall of different depths ($m^3/s/m$)

Cutoff Wall Length, X (m)	Present Study
0	$7.6502x\ 10^{-5}$
7	$5.4336x\ 10^{-5}$
8	$5.1689x\ 10^{-5}$
9	$4.9176x\ 10^{-5}$
10	$4.6780x\ 10^{-5}$
11	$4.4495x\ 10^{-5}$
12	$4.2311x\ 10^{-5}$

3. Conclusion

In this study, seepage analysis of the embankment dam body and its foundation is investigated using the FEM based on Galerkin's approach. By writing a program in Fortran language, hydraulic head, pressure values and quantity of seepage are found at the dam body and foundation points.

It has been concluded that permeability in the x-direction is more effective on the seepage amount in fill dams.

The presence of horizontal drainage is important for the downstream region.

The seepage rate increases as the horizontal drainage length increases.

The cutoff lengthens the seepage length and reduces the permeability seepage rate per unit width.

Acknowledgements

The authors thank the Scientific Research Projects Directorate of Cukurova University for supporting the present study (FBA-2019-12058).

References

[1] Ardıçlıoğlu, M. (1990). Sonlu elemanlar yöntemi ile Aslantaş baraj gövdesinde sızma analizi, Master thesis, Cukurova University, Turkey. (In Turkish)

[2] Keskin, S. B. (2005) Toprak dolgu baraj gövdesindeki ve altındaki sızma olayının incelenmesi, Master thesis, Pamukkale University, Turkey. (In Turkish)

[3] Çilingir, H. (2007) Toprak Dolgu barajların gövdelerindeki sızmaların sonlu elemanlar yöntemi ile incelenmesi: Büyükçekmece barajı uygulaması, Master thesis, Istanbul Technical University, Turkey. (In Turkish)

[4] Fakhari, A., Ghanbari, A. (2013). A Simple method for calculating the seepage from earth dams with clay core. Journal of GeoEngineering, 8, 27-32.

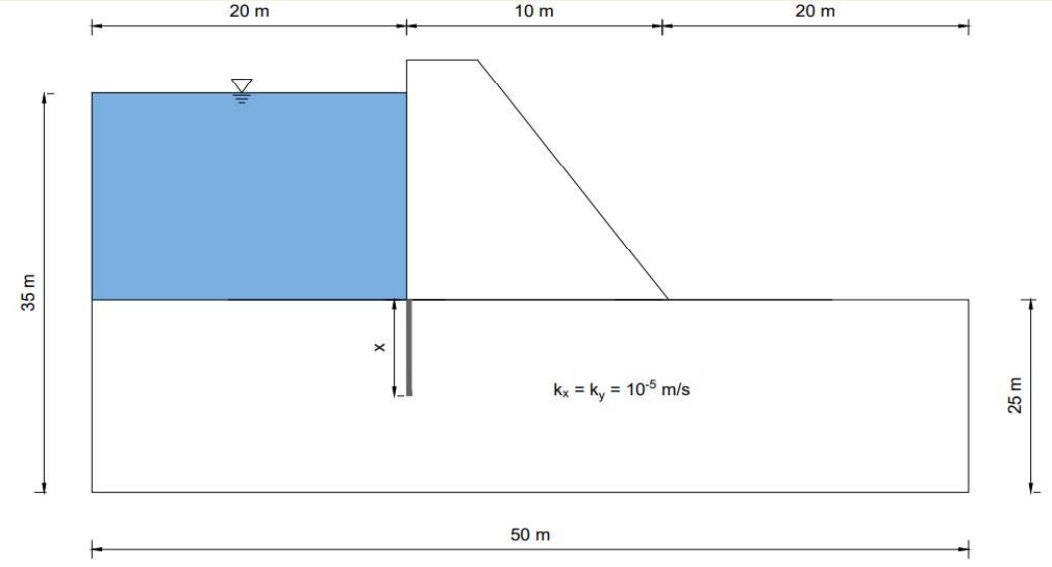

Figure 10. Geometry and material properties of the dam with cutoff wall (Example 6)

[5] Çelik, B. (2014)Aydın İkizdere barajı sonlu elemanlar yöntemi ile sızma analizi, Master thesis, Gazi University. (In Turkish)

[6] Sağlıca, O. (2013) Dolgu baraj gövdelerinde sızma analizi, Master thesis, Gazi University, Turkey. (In Turkish)

[7] Darbandi, M., Torabi, S., Saadat, M., Daghighi, Y., Jarrahbashi D., (2007). A Moving-Mesh finite-volume method to solve free-surface seepage problem in arbitrary geometries. Int. J. Numer. Anal. Meth. Geomech, 31 1609–1629.

[8] Rafıezadeh, K., Ataıe-ashtiani, B. (2013). Seepage analysis in multi-domain general anisotropic media by three-dimensional boundary elements. Engineering Analysis with Boundary Elements, 37, 527–541.

[9] Ourıa, A., Toufıgh, M.M., (2009). Application of nelder-mead simplex method for unconfined seepage problems. Applied Mathematical Modelling, 33, 3589–3598.

[10] El-Jumaıly, K.K., Al-bakry, J.M.H, (2013). Seepage analysis through and under hydraulic structures applying finite volume method. Eng. Tech.J., 9, 1719-1731.

[11] Mesci, S.B. (2006). Dolgu baraj gövdelerindeki sızmaların ve freatik hattın incelenmesi: seferihisar barajı uygulaması, Master thesis, Istanbul Technical University, Turkey. (In Turkish)

[12] Çakır, H.U. (2011). Yeraltısuyu akımlarının modellenmesinde kollokasyon metodu, Master thesis, Dokuz Eylul University, Turkey. (In Turkish)

[13] Quanshu, L., Jianjun, L., (2010). Numerical analysis of the seepage field in core-dam Iı quanshu, LIU Jianjun 492-499. https://www.researchgate.net/publication/267976261_Numerical_Analysis_of_the_Seepage_Field_in_Core-Dam.

[14] Mansuri, B., Salmasi, F., (2013). Effect of horizontal drain length and cutoff wall on seepage and uplift pressure in heterogeneous earth dam with numerical simulation. Journal of Civil Engineering and Urbanism, 3(3), 114-121.

[15] Sakhmarsi, A.A., Akhbari, H., Naeimi, S.P., Kiapey, A. (2014). The effect of the cutoff wall conditions on the seepage characteristics of homogeneous earth-fill dams using SEEP/W. WALIA journal, 30(S2), 176-182.

[16] Yuan, S., Zhong, H., (2016). Three dimensional analysis of unconfined seepage in earth dams by the weak form quadrature element method. Journal of Hydrology, 533, 403–411.

[17] Zhang, W., Dai, B., Liu, Z., Zhou, C. (2017). Unconfined seepage analysis using moving kriging mesh-free method with Monte Carlo integration. Transport in Porous Media, 116(1), 163–180.

[18] Khassaf, S.I., Madhloom A.M.,(2017). Efect of impervious core on seepage through zoned earth dam (case study: Khassa Chai dam). Int J Sci Eng Res.,8(2),1053–1064.

[19] Zewdu, A., (2019), Seepage and slope stability analysis of earthen dam: a case study of Koga Dam. Ethiopia, WNOFNS, 26, 191-217.

[20] Taghvaei, P., Mousavi, S.F., Shahnazari, A., Karami, H., Shoshpash, I. (2014). Experimental and numerical modeling of nano-clay efect on seepage rate in earth dams. Int J Geosynth Ground Eng., 5(1),1.

[21] Doaa, A., El Molla, T. (2019), Seepage through homogeneous earth dams provided with a vertical sheet pile and formed on impervious foundation. Ain Shams Eng J., 10(3), 529–539.

[22] Sanayei, H.R.Z., Javdanian, H. (2020). Assessment of steady-state seepage through dams with nonsymmetric boundary conditions: analytical approach, Environ Monit Assess, 192: 3.

[23] Salmasi, F., Nouri, M., Abraham J.(2020). Upstream cutoff and downstream filters to control of seepage in dams. Water Resources Management, 34, 4271–4288.

[24] Kheiri, G., Javdanian, H., Shams, G. (2020). A numerical modeling study on the seepage under embankment dams, Modeling Earth Systems and Environment, 6, 1075–1087.

[25] Doorı, S., Noorı, A. R. (2021). Finite element approach for the bending analysis of castellated steel beams with various web openings, ALKÜ Fen Bilimleri Dergisi, 3 (2), 38-49.

[26] Chai, Y., Li, W., Liu, Z., (2022). Analysis of transient wave propagation dynamics using the enriched finite element method with interpolation cover functions, Applied Mathematics and Computation, 412, 126564.

[27] Pinnola, P.F., Vaccaro, M.S.,Barretta, R., Sciarra, F.M., (2022). Finite element method for stress-driven nonlocal beams, Engineering Analysis with Boundary Elements,134, 1,22-34.

[28] Ma, S., Chen, M., Skelton, R.E. (2022).Tensegrity system dynamics based on finite element method, Composite Structures, 280, 114838

[29] Ming, H.,Yun, L.L., Shuai, Z., Zhang, A.M. (2022). Research on characteristics of deep-sea implosion based on Eulerian finite element method, Ocean Engineering, 110270.

[30] Harr, A. E. (1962). Groundwater and Seepage, McGRaw-Hill Book Company, 1962.

[31] Jie, Y.-x., Liu, L., Xu, W., Li, G., (2013). Application of NEM in seepage analysis with a free surface. Mathematics and Computers in Simulation, 89, 23–37.

[32] Noori, A.R., Aslan, T.A., Temel, B. (2019). Dairesel plakların sonlu elemanlar yöntemi ile laplace uzayında dinamik analizi. Niğde Ömer Halisdemir Üniversitesi Mühendislik Bilimleri Dergisi, 8(1), 193-205. (In Turkish)

[33] Parsi, M. J. K., Daneshm, F., (2012). Unconfined seepage analysis in earth dams using smoothed fixed grid finite element method. Int. J. Numer. Anal. Methods Geomech., 36, 780–797.

[34] Parsi, M.J.K., (2019). Isogeometric analysis in solution of unconfined seepage problems. Computers and Mathematics with Applications, 78, 66–80.

[35] Mansuri, B., Salmasi, F., Oghati. B., (2014). Effect of location and angle of cutoff wall on uplift pressure in diversion dam, Geotech Geol Eng., 32,1165–1173.